

## PARAMETRIC STUDY ON THE SPRING-BACK EFFECT IN AA5052 ALLOY IN THE COURSE OF THREE-POINT ROLL BENDING PROCESS

Viswanathan SHRINAATH,\*Ramalingam VAIRAVIGNESH,\*Ramasamy PADMANABAN\*

\*Department of Mechanical Engineering, Amrita School of Engineering, Coimbatore, Amrita Vishwa Vidyapeetham,  
 Amritanagar, Coimbatore - 641 112 Tamil Nadu, India

[anand.shri96@gmail.com](mailto:anand.shri96@gmail.com), [r\\_vairavignesh@cb.amrita.edu](mailto:r_vairavignesh@cb.amrita.edu), [dr\\_padmanaban@cb.amrita.edu](mailto:dr_padmanaban@cb.amrita.edu)

*Received 25 December 2019, revised 13 October 2020, accepted 16 October 2020*

**Abstract:** Three-point roll bending is one of the most common forming processes employed to obtain the desired radius of curvature in the sheet metal operations. Upon the removal of the forming load, the sheet metal deforms to a lesser extent than that of the required dimension. This phenomenon is termed as spring-back and is considered the most challenging areas of research in three-point roll bending of sheet metals. This study aims to develop a numerical model using HyperWorks and Radioss solver to understand the influence of load, the distance between the forming rollers, and its thickness on the spring-back effect in the course of three-point roll bending of sheet metal (AA5052). The results of the numerical model are validated with the results of the experimental trials. Besides, a statistical model is developed to relate the amount of spring-back with the three-point roll bending process parameters.

**Keywords:** Three-point roll bending, multi-pass forming process, spring-back, dynamic explicit analysis, optimization

### 1. INTRODUCTION

AA5052 is an aluminum alloy with magnesium as the primary alloying element and is known for its high corrosion resistance and low weight to high strength ratio. Hence, it is widely used in aircraft tubes, automobile parts, and hydraulic tubes. Besides, AA5052 alloy has good formable properties. However, the forming of AA5052 alloy has many challenges. Sheet metal forming is one of the important and most common processes used in the manufacturing industries (Hecker, 1975; Hu et al., 2002; Parsa et al., 2012). During forming processes, force is applied on the sheet metal to modify its geometry rather than the removal of material. Three-point roll bending is one of the forming processes, which bends a long continuous strip of sheet metal into a large or medium size tubular section that is typically used in aircraft structures, pressure vessels, and tunnels.

The symmetric roll bending machines have three rollers with an arrangement similar to that of an isosceles triangle. In symmetric roll bending machines, the top roller moves vertically, and the bottom rollers move horizontally. The vertical movement of the roller applies a load on the sheet metal. The rotation of bottom rollers helps in uniform distribution of the load along the length of the sheet metal, forming the sheet metal to the desired radius of curvature. However, the recovery of the elastic region in the sheet metal upon removal of load results in the spring-back effect. The forming of the sheet metal to the desired radius of curvature depends on the thickness of the sheet metal, material property (Young's modulus, Poisson's ratio & yield strength), and the process parameters such as displacement of the top roller (TRD), the distance between the bottom rollers (DBBR), the radius of top and bottom roller.

A few studies attempted to understand the behavior of the

sheet metal during the forming process (Abvabi et al., 2014; Ghimire et al., 2017; lee et al., 2005; Westermann et al., 2011; Xing et al., 2013; Xu et al., 2004; Belykh et al., 2016; Davies and Magee, 1977; Fortin et al., 1983; Kumar et al., 2014). Hansen and Jannerup(1979) developed an analytical model to predict the final curvature (range) of the sheet metal. The results indicate that the final curvature is highly sensitive to the forming parameters than that of the material properties. However, the analytical model predictions could not determine the exact final curvature. Hardt et al. (1982) developed a shape controller system for the forming process. The shape controller attains the desired shape based on the loaded sheet metal, material properties at the loaded position, and the amount of elastic spring-back. A series of experiments were conducted with a shape controller to attain the desired shape. However, the dynamic control of the workpiece was highly challenging with the shape controller.

Yang and Shima(1988) determined the relationship between the displacement of the center roller and the final curvature of the sheet metal in the forming process. He also demonstrated that the distribution of the curvature was axisymmetric about a point and was not symmetric about the center of the axis. However, material properties were not considered in the analytical method. Gandhi and Ravel (2006) developed models for single-pass bending with constant Young's modulus and multi-pass bending with constant and varying Young's modulus. However, the study lacks a comprehensive analysis of the influence of the number of passes and the load applied. Srivastav and Shinde (2010) studied the dynamic process of the plate rolling using finite element analysis. A 3D, dynamic elastic-plastic for steel material, was developed and validated to study the stress and strain in the sheet metal using Radioss. However, the influence of parameters was not discussed explicitly.

A few analytical models were developed to analyze the spring-

back effect in the three-point roll bending of aluminum alloys (Yang and Shima, 1988; Paulsen and Welo, 1996; Badr et al., 2017; Guo et al., 2017; Ameen, 2012; Liu et al., 2018; Ktari et al., 2012; Khamen et al., 2016). However, these models were developed based on the theory of bending in which the neutral axis remains at the midpoint along with the thickness and the material properties like Young's modulus remaining constant for the entire process. However, in practical situations, Young's modulus changes while deforming the material to the desired shape.

Most of the studies were carried out using finite element models to correlate the process parameters with the experiment results (final radius of curvature). Finite element analysis to investigate the effect of process parameters on the spring-back effect during deformation processing of materials is not available in the open literature.

The study aims to perform a parametric study on the three-point roll bending process and spring-back effect in the materials. A simulation model was developed for the three-point process using HyperWorks(2010) and Radioss(2014). The model was validated using the experimental test. The influence of process parameters in three-point roll bending on the spring-back effect was analyzed using a hybrid linear and radial basis function model. The model was used to optimize the process parameters to achieve the minimum spring-back effect (desired radius of curvature).

## 2. MATERIALS AND METHODS

### 2.1. Computational Methodology

Computation methodology is a powerful and cost-effective tool used to predict the approximate solution for practical problems. In this work, the finite element method and design of experiments are used to explore the amount of spring-back in the three-point roll bending process.

#### 2.1.1. Numerical Modeling

Non-linear dynamic finite element model was developed to predict the large plastic strain, large deformation, and contact phenomenon during the three-point roll bending process of the sheet metal. The finite element model was developed using HyperWorks(2010) and solved using a Radioss solver (2004). The bending process of sheet metal was simulated using the explicit analysis while the spring back process used the implicit analysis. The developed finite element model used a multi-stage forming process, where the top roller displacement was given stage-wise to achieve the accuracy of the formed radius of curvature. The accuracy of the developed model depends on the contact properties between roll and sheet metal. The mid-surface of the sheet metal was extracted to reduce the computation time and the results were calculated along the mid-surface normal.

#### 2.1.2. Geometric Specification

The 3D solid model of three rollers and the sheet metal was developed, based on the three-point roll machine specification process condition given in Table 1.

Tab. 1. Geometric specification

Parameters	Dimension in mm
Top roller diameter	220
Bottom roller diameter	140
Distance between the bottom rollers	380
Sheet metal dimension	900×100×3

### 2.1.3. Meshing and Element Properties

The 3D model of the three-point roll bending process was imported and was meshed using Hypermesh. The roller and sheet metal were meshed using 2D first order quadrilateral element of element length 10 mm as shown in Figure 1. The sheet metal elements were modeled as orthotropic shell elements with an angle of 0° degree. The QEPH Shell element would auto-stabilize hourglass energy. The shell element properties were as follows: the thickness of sheet metal = 3 mm, number of integration point (N) = 5, lthick = 1, and lplastic = 1. Since the roller is a rigid body, three rigid elements were created for each roller using the RB2 element. RB2 element has one independent node at the center and all other nodes are dependent nodes connected to the independent node.

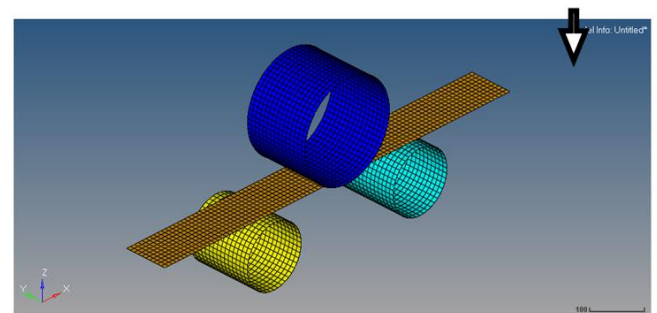


Fig. 1. Meshed model

### 2.1.4. Material Properties

The rollers were made of steel while the sheet metal was made of AA5052 alloy of thickness 3 mm. Since the sheet metal was deforming plastically in an anisotropic way, elastoplastic Hill's model (Hill, 1958) was used to define the shell element of the sheet metal. The material properties like Young's modulus, Poisson ratio, and density were given as input.

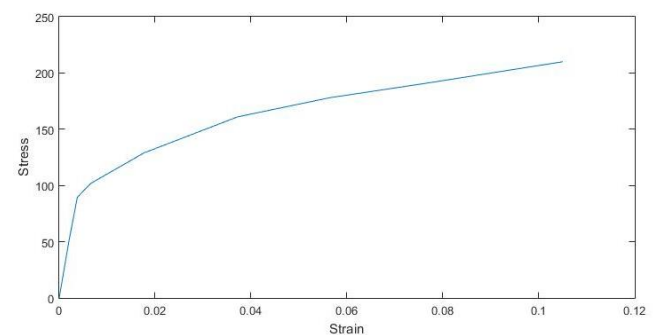


Fig. 2. True stress (MPa) – strain (ratio; no units) curve of Aluminum 5052

In this elastoplastic model, the effective stress-strain curve of Aluminum 5052 and Lankford formability constant was given as an input following the studies of Hecker (1975). The anisotropic coefficients (plastic strain ratio; no units) are as follows:  $R_0 = 0.74$ ,  $R_{45} = 0.48$ , and  $R_{90} = 1.04$ . Figure 2 shows the true stress-strain curve of AA5052.

**2.1.5. Load and Boundary Conditions**

The forming process was accomplished in two-steps, the first step is bending, that is, the load is given to the sheet metal by the displacement of the top roller and the second step is rolling, that is, the rollers rotate to distribute the load along the length of sheet metal. Hence, the constraints of the rollers were given to the independent nodes of the rigid element (RB2), all the dependent node would take the constraints given to the independent node. The constraints were given in the global axis, for the top displacement along the X3 axis, and rotation along the X2 axis was allowed. Similarly, for the bottom roller, only rotation along the X2 axis was allowed. Since this forming process is a multi-stage process, for each displacement of the top roller, the bottom roller rotates at 0.000785 rad/ms. The top roller was displaced 8 times by 5 mm totaling a displacement of 40 mm.

**2.1.6. Contact Definition**

In the finite element analysis, the Master-Slave approach was used to define the contact in the model. Since the surface of the sheet metal made a contact with the rollers, the surface to surface contact was defined in the finite element model. Rollers were defined as the master nodes since it was a rigid body, and sheet metal as slave nodes. The interaction between the roller and sheet metal was assigned as a sliding approach because the sheet metal slides into the roller by the friction factor. In this model, the friction is assumed to be a constant of 0.1. The gap between the sheet metal and roller was set constant because of no considerable change in the thickness of the sheet metal.

**2.1.7. Spring-Back Procedure**

Spring back is the recovery of the elastic region when the applied load is removed. For the spring back process, a separate engine file was created, and it was carried out as an implicit analysis. The spring back engine file would start after the termination time of the dynamic forming process.

**2.2. Statistical Model**

A manufacturing process is analyzed based on the process parameters, as the process parameters significantly influence the properties/geometries of the product. Conducting experimental/numerical trials for analyzing the influence of process parameters is a time-consuming process. Hence, the study adopted the Design of Experiments approaches to minimize the number of trials to study the influence of process parameters on the spring-back effect.

In this study, three factors namely top roller displacement

(TRD), the distance between bottom rollers (DBBR), and sheet metal thickness (Thick) were varied at five levels. The numerical simulations were carried out based on the parametric combinations, given in Table 2. The finite element model was used to predict the amount of spring-back (geometry changes of the sheet metal before and after spring-back) in the roll forming process. A hybrid linear function and radial basis function was developed to correlate the process parameters with the amount of spring-back. The development of the hybrid linear function and radial basis function-based model is based on the previous literature (Ramalingam and Ramasamy, 2017; Vignesh et al., 2018; Vignesh and Padmanaban, 2018). The model was used to develop contour plots, which in turn were used to study the interactive effect of process parameters on the amount of spring-back in three-point roll bending of AA5052 alloy.

Tab. 3. Design Matrix

Sl. No.	Process Parameters						Amount of Spring Back (mm)*
	Real Value			Coded value			
	Thick (mm)	TRD (mm)	DBBR (mm)	Thick	TRD	DBBR	
1	1	40	380	-2	0	0	750
2	2	40	380	-1	0	0	345
3	3	30	380	0	-2	0	400
4	3	35	380	0	-1	0	270
5	3	40	360	0	0	-2	117
6	3	40	370	0	0	-1	150
7	3	40	390	0	0	1	218
8	3	40	400	0	0	2	258
9	3	45	380	0	1	0	130
10	3	50	380	0	2	0	100
11	4	40	380	1	0	0	140
12	5	40	380	2	0	0	100

\*Geometry changes of the sheet metal before and after spring-back

**2.3. Experimental Methodology**

The three-point roll bending trials on AA5052 sheet metal were performed on the symmetrical three-point roll bending machine. The machine specification and the sheet metal specification are given in Table 1. In symmetrical three-point roll bending, the AA5052 alloy sheet metal was placed in such a way that the load will be acting on the midpoint of the sheet metal. Before applying the load, it was ensured that all the three rollers made contact with the sheet metal. The initial position of the top roller was noted and the top roller displacement was applied in steps. The top roller was displaced by 5 mm by the controller. Now at 5 mm of top roller displacement, the rotation velocity of 0.785 rad/s was given to the bottom rollers.

As the bottom roller rotated, the sheet metal moved in a horizontal direction because of the friction between the roller and the sheet metal. The bottom roller was rotated in both directions so that the direction could be reversed. The action was repeated until the load acted all over the sheet metal and until the top roller displaced up to 40 mm.

While removing the load, the sheet metal would spring-back until the equilibrium was achieved between the elastic and plastic

regions in the sheet metal. By the spring-back effect, the radius formed by the top roller increases as soon as the top roller is moved back to the initial position. This geometry changes of the sheet metal before and after spring-back is measured as the amount of spring-back. By the experimental test, only the radius of the sheet metal after the spring-back is measured, which is known as the final radius of the sheet metal after the spring-back. The bend region length and the radius after spring-back were as follows: bend region length = 430 mm and radius after spring-back = 660 mm. Since the experiment was carried out without the pre-bending, the bend region was taken into consideration.

putation time. A poor mesh that has a large aspect ratio of the element, leads to inaccurate prediction or convergence problems. However, refining the mesh considerably increases the computation time. A Mesh convergence study for the sheet metal was performed. The results indicate that that the load transfer was almost the same for 10 mm and 8 mm element length. But the computational time was high for 8 mm element length. So, an element size of 10 mm was used for the study, as the predicted results were in good agreement with the experimental results.

### 3. RESULTS AND DISCUSSIONS

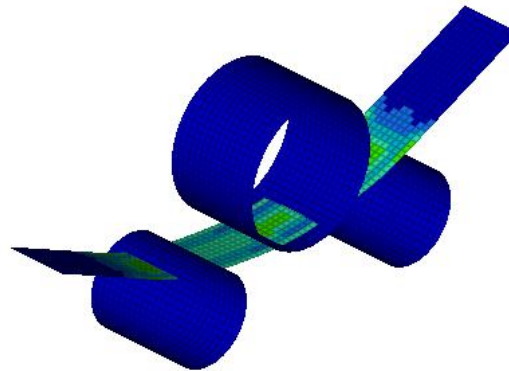
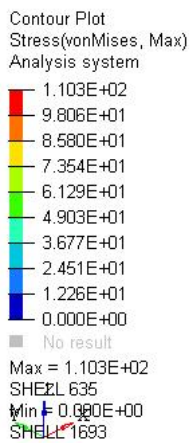
#### 3.1. Numerical Model

##### 3.1.1. Mesh Convergence

A finite element model with sufficient mesh density was used in this study. A convergence study was performed with different mesh densities, as it affects stress, displacement, and CPU com-

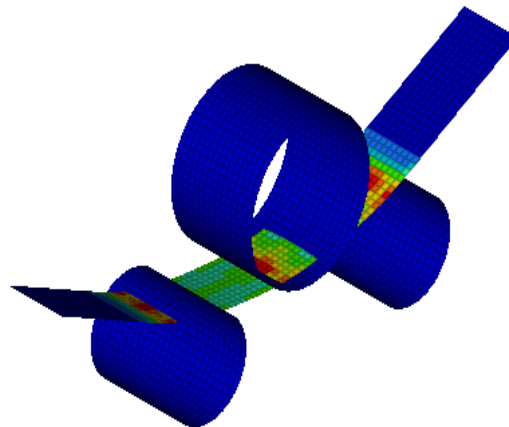
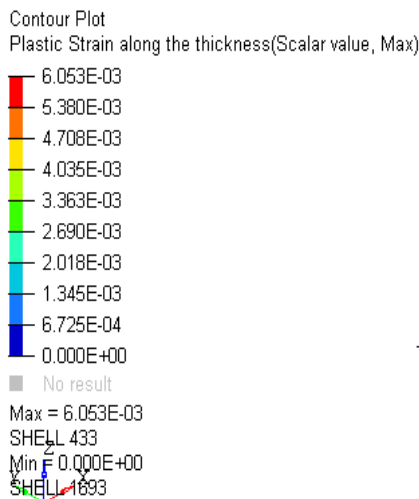
#### 3.1.2. Model Validation

The 2D finite element model was simulated based on the experimental data. The following results were obtained: stress distribution, strain distribution, deformation before and after spring-back, radius before spring-back, and after spring-back. Figure 3 shows the stress distribution in the sheet metal. The results indicate that plastic deformation occurred in the sheet metal when stress crossed the yield limit. Based on this stress distribution, the plastic strain developed in the sheet metal is shown in Figure 4.



1: PLATE  
Loadcase 1 : Time = 1.5000e+005 : Frame 6830

Fig. 3. Stress (MPa) distribution in the sheet metal



1: PLATE  
Loadcase 1 : Time = 1.5000e+005 : Frame 6830

Fig. 4. Plastic strain (ratio; no units) distribution in the sheet metal

When the top roller contact was removed, the sheet metal underwent spring-back, that is, recovery of the elastic region in the material. If spring-back occurred, the radius of the deformed sheet metal was either higher or lower than that of the desired radius. The curvature of the sheet metal before spring-back was 507 mm and the curvature of sheet metal after spring-back 635 mm.

Table 3 shows the final radius of curvature after spring back from the finite element model and experimental test. The numerically predicted the final radius of curvature of the sheet metal was in good correlation with the experimental results.

Tab. 3. Model validation with Experimental test

	Simulation Result	Experimental Result
Radius after spring back (mm)	635	660

### 3.2. Statistical model

Table 2 shows the design matrix for variation in the process parameters and the corresponding spring-back. The process parameters (top roller displacement, the distance between bottom rollers, the thickness of sheet metal) are related to the response (amount of spring-back) using a hybrid linear-radial basis function model. The generated statistical model is a hybrid Linear-Radial Basis Function, that is given by equation (1). The Radial Basis Function network was developed using a multiquadric kernel with 4 centers, global width of 0.24811 and a regularization parameter, and a lambda of 0.0001.

$$T = 118.2636 - 224.9054 * DBBR - 258.9317 * TRD - 924.9986 * Thickness + RBF \quad (1)$$

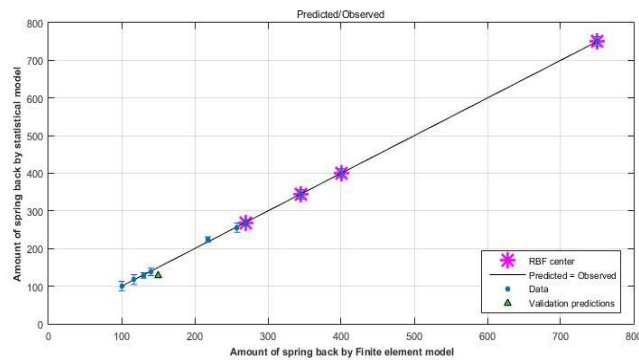


Fig. 5. Amount of spring back (mm) – Finite element model vs Statistical model

From Figure 5, a linear trend was observed between the amount of spring-back from the finite element model and the predicted statistical model. The coefficient of determination (R2) and root mean squared error (RMSE) value was used to assess the efficiency of the developed statistical model. The R2 was 1 for the statistical model, depicting its closeness with the finite element model predictions. The RMSE is 4.137 for the statistical model, which is small.

### 3.2.1. Effect of Process Parameters

The effect of TRD and the DBBR on the amount of spring back is shown in Figure 6. The material deformed at 30 mm TRD and 360 mm DBBR exhibited the largest spring-back. The amount of spring back reduced as the DBBR increased from 360 mm to 380 mm. With the further increment in DBBR from 380 mm to 400 mm, the amount of spring back increased. Similarly, if TRD increased, the amount of spring back decreased. The force exerted on the sheet metal for 30 mm of TRD was 260 N.

Correspondingly, the stress of 104.3 MPa and strain of 3.54e-03 was induced in the sheet metal. With an increase in TRD to 50 mm, the force exerted on the sheet metal was 310 N. The corresponding stress in the sheet metal was 115.7 MPa, and strain in the sheet metal is 8.0e-03. The developed strain lay well enough in the plastic region, which was higher than that of the strain developed with TRD of 30 mm. Besides, the amount of spring-back in the sheet metal reduced with more plastic deformation. Hence, spring-back decreased with an increase in TRD.

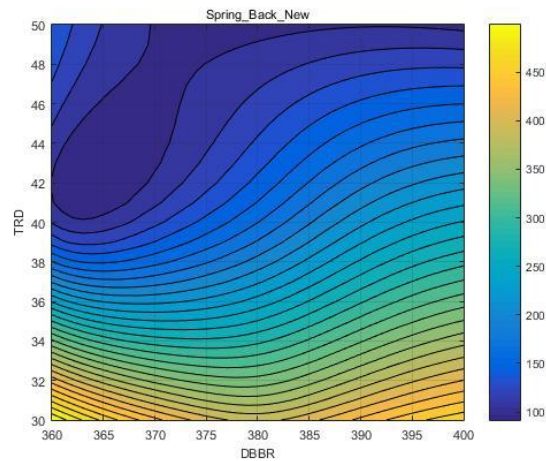


Fig. 6. Effect of top roller displacement (mm) vs distance between bottom rollers (mm) on spring-back (mm)

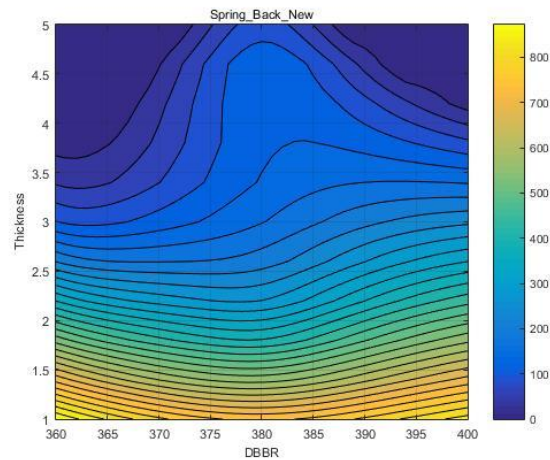


Fig. 7 Effect of the thickness (mm) vs distance between bottom roller (mm) on spring-back (mm)

The amount of spring-back was low for the sheet metal deformed at 40 mm TRD and 360 mm DBBR. As DBBR increased,

the amount of spring back also increased. The load applied by the top roller acted over a narrow region in the sheet if the DBBR was less (i.e., 360 mm). Hence, the stress and strain developed in the region were 113.2 MPa and 7.37e-03. With an increase in the load application area (DBBR > 360 mm), the stress-induced was 108.4 MPa, and the strain in the sheet metal was 5.02e-03. Hence, the sheet metal formed at 360 mm DBBR had lesser spring-back than that formed at 400 mm DBBR. A lesser amount of spring-back was observed in the sheet metal that was deformed at low DBBR and high TRD.

The effect of sheet metal thickness and DBBR on the amount of spring-back is shown in Figure 7. The sheet metal of thickness 1 mm deformed at 360 mm DBBR had the highest amount of spring-back. When the DBBR was increased from 360 mm to 380 mm, the amount of spring-back decreased. However, with a further increase in DBBR from 380 mm to 400 mm, the amount of spring back decreased. The amount of spring back reduced with an increase in the thickness of sheet metal. A force of 850 N was exerted on the sheet metal of thickness 5 mm that induced stress of 122.2 MPa and strain 1.10e-02. The developed strain was in the plastic region, as the stress was larger than the yielding stress of 89.5 MPa. Hence, the amount of spring-back was lesser. During deformation, a force of 24 N induced stress of 93.7 MPa and strain of 6.07e-04 in the sheet metal of thickness 1 mm. As the induced stress value was similar to the yielding stress of 89.5 MPa, a large amount of spring-back was observed in the sheet metal of thickness 1 mm than that of sheet metal of thickness 5 mm.

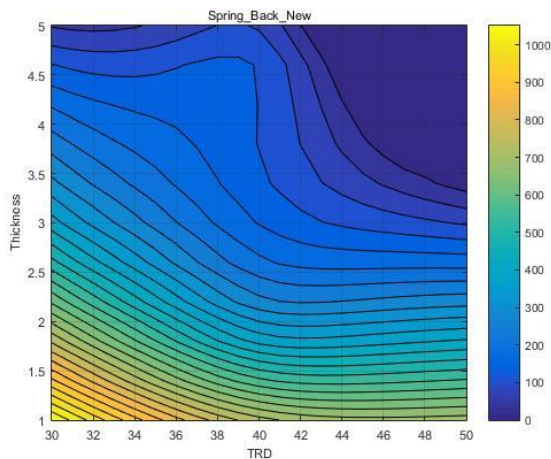


Fig. 8. Effect of thickness (mm) vs top roller displacement (mm) on spring-back (mm)

Tab.4.Optimized values

Sl. No.	Process Parameters	Values
1	Top roller displacement	42 mm
2	Distance between bottom rollers	385 mm
3	Sheet metal thickness	3.5 mm

From Figure 6 and Figure 7, it is observed that DBBR has a less significant effect on the amount of spring-back than that of TRD and sheet metal thickness. However, DBBR behaves uniquely if TRD and thickness of the sheet metal were low. The effect of sheet metal thickness and TRD is shown in Figure 8. It is

observed that the amount of spring-back was high for 1 mm sheet metal thickness and 30 mm TRD. As mentioned earlier, the amount of spring-back reduced with an increase in TRD from 30 mm to 50 mm. It is observed that the amount of spring-back was less when the sheet metal thickness was high, and the TRD was high. The optimization results are as shown in Table 4. If the roll forming process is performed at that level of process parameters, the spring-back effect was minimum. The optimization results were successfully validated with the finite element model.

#### 4. CONCLUSION

A finite element model was developed and validated to predict the amount of spring back in the roll forming process for AA5052 alloy. A linear-radial basis function model was developed interrelating the process parameters namely top roller displacement, the distance between bottom rollers, and thickness of the sheet metal with the amount of spring back. The model was utilized to optimize the process parameters to reduce the amount of spring back in the course of the roll forming process of AA5052 alloy. The results demonstrated the following:

- The amount of spring-back increases with an increase in top roller displacement.
- The amount of spring-back decreases with an increase in the thickness of the sheet metal.
- Distance between the bottom rollers has a minor influence on the spring-back effect.

#### REFERENCES

1. **Abvabi A., Mendiguren J., Rolfe B.F., Weiss M.** (2014), Springback Investigation in Roll Forming of a V-Section, *Applied mechanics and materials*, 553, 643–648.
2. **Ameen H.A.** (2012), Effect of Sheet Thickness and Type of Alloys on the Springback Phenomenon for Cylindrical Die, *American journal of scientific and industrial research*, 480.
3. **Badr O.M., Rolfe B., Zhang P., Weiss M.** (2017), Applying a new constitutive model to analyse the springbackbehaviour of titanium in bending and roll forming, *International Journal of Mechanical Sciences*, 128, 389–400.
4. **Belykh S., Krivenok A., Bormotin K., Stankevich A., Krupskiy R., Mishagin V., Burenin A.** (2016), Numerical and Experimental Study of Multi-Point Forming of Thick Double-Curvature Plates from Aluminum Alloy 7075, *KnE Materials Science*, vol (NA), 17–23.
5. **Davies R., Magee C.** (1977), *The effect of strain rate upon the bending behavior of materials*, ASME, New York.
6. **Fortin P., Bull M., Moore D.** (1983), *An optimized aluminum alloy (x6111) for auto body sheet applications*, SAE Technical Paper.
7. **Gandhi A., Raval H.**, (2006), Article Title, ASME 2006 International Mechanical Engineering Congress and Exposition, *American Society of Mechanical Engineers Digital Collection*, 107–116.
8. **Ghimire S., Emeerith Y., Ghosh R., Ghosh S., Barman R.N.** (2017), Finite Element Analysis of an Aluminium Alloy Sheet in a V-Die Punch Mechanism Considering Spring-Back Effect, *International Journal of Theoretical and Applied Mechanics*, 12, 331–342.
9. **Guo X., Gu Y., Wang H., Jin K., Tao J.** (2018), The Bauschinger effect and mechanical properties of AA5754 aluminum alloy in incremental forming process, *The International Journal of Advanced Manufacturing Technology*, 94, 1387–1396.
10. **Hansen N., Jannerup O.** (1979), *Modelling of elastic-plastic bending of beams using a roller bending machine*, ASME, New York
11. **Hardt D., Roberts M., Stelson K.A.** (1982), *Closed-loop shape control of a roll-bending process*, ASME, New York

12. **Hecker S.** (1975), *Formability of aluminum alloy sheets*, ASME, New York
13. **Hill R.** (1958), A general theory of uniqueness and stability in elastic-plastic solids, *Journal of the Mechanics and Physics of Solids*, 6, 236–249.
14. **Hu J., Marciniak Z., Duncan J.** (2002), *Mechanics of sheet metal forming*, Elsevier, Oxford.
15. **HyperWorks** (2010), *HyperMesh*, Version 11.
16. **HyperWorks** (2014), *Hyperworks 14.0 RADIOSS reference guide*, Altair engineering.
17. **Khamneh M.E., Askari-Paykani M., ShahverdiH., Hadavi S.M.M., Emami M.** (2016), Optimization of spring-back in creep age forming process of 7075 Al-Alclad alloy using D-optimal design of experiment method, *Measurement* 88, 278–286.
18. **Ktari A., Antar Z., Haddar N., Elleuch K.** (2012), Modeling and computation of the three-roller bending process of steel sheets, *Journal of mechanical science and technology*, 26, 123–128.
19. **Kumar K.D., Appukuttan K., Neelakantha V., Naik P.S.** (2014), Experimental determination of spring back and thinning effect of aluminum sheet metal during L-bending operation, *Materials & Design*, 56, 613–619.
20. **Lee M.-G., Kim D., Kim C., Wenner M.L., Chung K.** (2005), Spring-back evaluation of automotive sheets based on isotropic-kinematic hardening laws and non-quadratic anisotropic yield functions, part III: applications, *International journal of plasticity*, 21, 915–953.
21. **Liu Y., Wang L., Zhu B., Wang Y., Zhang Y.** (2018), Identification of two aluminum alloys and springback behaviors in cold bending, *Procedia Manufacturing*, 15, 701–708.
22. **Parsa M., Pishbin H., Kazemi M.** (2012), Investigating spring back phenomena in double curved sheet metals forming, *Materials & Design*, 41, 326–337.
23. **Paulsen F., Welo T.** (1996), Application of numerical simulation in the bending of aluminium-alloy profiles, *Journal of Materials Processing Technology*, 58, 274–285.
24. **Ramalingam V.V., Ramasamy P.** (2017), Modelling corrosion behavior of friction stir processed aluminium alloy 5083 using polynomial: radial basis function, *Transactions of the Indian Institute of Metals*, 70, 2575–2589.
25. **Srivastav Y., Shinde S.** (2010), Dynamic Simulation and Analysis of Plate Roll Bending Process for Forming a Cylindrical Shell, *Proceedings of the HyperWorks Technology Conference 2010*, Altair Technology Conference.
26. **Vignesh R.V., Padmanaban R., Datta M.** (2018), Influence of FSP on the microstructure, microhardness, intergranular corrosion susceptibility and wear resistance of AA5083 alloy, *Tribology-Materials, Surfaces & Interfaces*, 12(3), 157–169.
27. **Vignesh V., Padmanaban R.** (2018), Modelling of peak temperature during friction stir processing of magnesium alloy AZ91, *IOP Conference Series: Materials Science and Engineering*, 310(1), 012019.
28. **Westermann I., Snilsberg K.E., Sharifi Z., Hopperstad O.S., Marthinsen K., Holmedal B.** (2011), Three-point bending of heat-treatable aluminum alloys: influence of microstructure and texture on bendability and fracture behavior, *Metallurgical and Materials Transactions, A* 42, 3386–3398.
29. **Xing M.-Z., Wang Y.-G., Jiang Z.-X.** (2013), Dynamic fracture behaviors of selected aluminum alloys under three-point bending, *Defence Technology*, 9, 193–200.
30. **Xu W., Ma C., Li C., Feng W.** (2004), Sensitive factors in springback simulation for sheet metal forming, *Journal of Materials Processing Technology*, 151, 217–222, (2004).
31. **Yang M., Shima S.** (1988), Simulation of pyramid type three-roll bending process, *International Journal of Mechanical Sciences*, 30, 877–886.

Acknowledgment: The authors express their sincere gratitude to Mr. Ashutosh Sinha, Senior Engineer, System Design and Detail Engineering Department, Larsen & Toubro Limited (Defense), Coimbatore for his guidance and support to perform numerical and experimental tests.